Crystal-field excitations and magnetic properties of Ho^{3+} in $HoVO_4$

S. Skanthakumar, C.-K. Loong, and L. Soderholm
Intense Pulsed Neutron Source and Chemistry Division, Argonne National Laboratory, Argonne, Illinois 60439-4814

M. M. Abraham and L. A. Boatner
Solid State Division, Oak Ridge National Laboratory, Oak Ridge, Tennessee 37831-6056
(Received 31 August 1994; revised manuscript received 26 January 1995)

The magnetic excitations in $HoVO_4$ were studied by neutron scattering and susceptibility techniques. Well-defined transitions between the crystal-field-split states of the Ho^{3+} ions were observed at 15, 40, and 100 K. The magnetic spectra were analyzed using a single-ion crystal-field model which includes intermediate coupling of the LS states of Ho. A quantitative comparison of the observed energies and intensities with the model was made and used to refine the five crystal-field parameters needed to calculate the Ho ionic wave functions and other magnetic properties. The nonmagnetic Γ_1-singlet ground state (containing about 90% pure $|8,0\rangle$ component) of the Ho ions, in conjunction with the next higher doublet state situated at 2.5 meV, strongly influences the low-temperature magnetic behavior. The calculated magnetic susceptibility, which exhibits an easy plane coinciding with the crystallographic *a-b* plane at low temperatures, agrees very well with the experimental data obtained from single-crystal measurements. The magnetic properties of $HoVO_4$ are contrasted with those of an isostructural compound $HoPO_4$ which has a 98% pure $|8,7\rangle$-doublet ground state. The difference in the crystal-field-level structure between these two compounds is reflected in a sign change of the B_0^2 crystal-field parameter. Despite the overall tetragonal crystal structure of $HoVO_4$, which predicts double degeneracy for each Γ_5 state, a small splitting in the first-excited doublet was clearly observed at low temperatures.

I. INTRODUCTION

Rare-earth orthovanadates form an isostructural series of compounds, RVO_4 (R=all rare-earth elements except La and including Sc and Y), with the tetragonal zircon structure (space group $I4_1/amd$).[1] This crystal structure contains a unique rare-earth site of D_{2d} point-group symmetry; and optically transparent, chemically stable, and mechanically robust nonmagnetic crystals such as YVO_4 and $LuVO_4$ often provide an effective host lattice for rare-earth-dopant-activated luminescence. For example, the use of Ho-doped YVO_4 crystals as a laser medium and Eu-doped YVO_4 as a phosphor for display devices has been proposed.[2,3] As the rare-earth concentration increases toward the stoichiometric composition RVO_4, interactions between neighboring rare-earth moments via indirect exchange may lead to long-range magnetic ordering, and in some materials, the $4f$-electron-phonon coupling can result in lattice instabilities or cooperative Jahn-Teller phase transitions.[4,5] A knowledge of crystal-field effects on the rare-earth ions and the interaction, if any, of these ions with the crystal lattice are essential to achieving an understanding of the optical and magnetic behavior of these materials.

The crystal-field splitting of $HoVO_4$ has been studied previously by means of a variety of experimental methods which included optical spectroscopy,[6–9] magnetic susceptibility[10] and magnetization measurements,[11,12] nuclear magnetic resonance,[13] and ultrasonic determinations of the elastic constants.[14] Unfortunately, susceptibility and magnetization measurements are not sufficiently sensitive to reveal the crystal-field structure, and an analysis of elastic-constant data requires the use of an additional model to account for magnetoelastic effects. Additionally, optical and NMR spectra do not provide the information necessary to resolve the upper states in the Ho^{3+} electronic ground multiplet. Perhaps for these reasons, the crystal-field energy-level schemes of $HoVO_4$, as presented by various workers,[6–8,10,11,14] vary considerably in the region above 50 cm^{-1}. (Note that 8.066 cm^{-1} is equivalent to 1 meV. These two units will be used interchangeably in the present paper.) The nonmagnetic-singlet ground state, which is separated from the next higher state by about 2.5 meV, has, however, been confirmed in all of the prior experiments. As a result, the Ho electronic moments do not order down to the mK range. Rather, antiferromagnetic ordering of the Ho nuclear spins, induced by an enhanced hyperfine interaction, occurs at 4.5 mK.[13,15–18] It should be noted that much of the early research on the low-temperature properties of $HoVO_4$ were driven by an interest in developing nuclear-cooling materials.

Achieving an understanding of the magnetic behavior of $HoVO_4$ over the 0–300 K temperature range requires a quantitative characterization of the magnetic-excitation spectrum as extended to high energies. In a previous study[19] of $HoPO_4$, we demonstrated that neutron-scattering studies can provide a complete description of the crystal-field-split ground multiplet of the Ho^{3+} ions, and thereby, provide a basis for the calculation of the magnetic susceptibility and specific heat. In a combined analysis of both the neutron and optical data, electronic

transitions up to 11 000 cm^{-1} can be satisfactorily accounted for by an empirical Hamiltonian, which contains the free-ion and crystal-field terms, using a total of 24 parameters. In this paper, we present the results of a related crystal-field study of $HoVO_4$. With the absence of conduction electrons in both RVO_4 and RPO_4, lattice vibrations are the primary excitations responsible for the nonmagnetic thermodynamic properties of these materials; and information concerning the dynamics of electrons and atoms is required for the interpretation of Jahn-Teller effects, lattice instabilities, and other magnetomechanical properties. A neutron-scattering study of the anomalous thermal expansion observed for both $HoVO_4$ and $HoPO_4$ will be given in another work.[20]

II. EXPERIMENTAL DETAILS

About 45 g of a polycrystalline-powder sample of $HoVO_4$ was prepared by a precipitation technique described elsewhere.[21] Neutron-scattering experiments were carried out at the Intense Pulsed Neutron Source at Argonne National Laboratory. Neutron-diffraction measurements confirmed the single-phase tetragonal zircon structure (space group $I4_1/amd$) of $HoVO_4$ over the temperature range of 12–300 K (typical Rietved weighted R factor $\approx 5.4\%$).[20] Inelastic neutron experiments were performed using the High-Resolution Medium-Energy Chopper Spectrometer (HRMECS). In the neutron energy-loss region, the resolution of the HRMECS spectrometer in full width at half maximum varies between 2 and 4 % of the incident-neutron energy.[22]

Data were collected for a wide range of momentum transfers (Q), and the observed data in the inelastic region include magnetic (mainly crystal-field transitions) and nuclear (mainly phonon) scattering. The differentiation between the nuclear and the magnetic components was made based on a comparison with the corresponding spectra of the isostructural nonmagnetic compound $LuVO_4$ and on a temperature- and Q-dependence study of the data. Such procedures, as well as those for the background corrections and intensity normalization, are well established and have been fully described in previous studies.[19,23–25] A closed-cycle helium refrigerator was used to cool the sample, and the measurements were made at 15, 40, and 100 K with incident energies of 5, 20, 50, and 200 meV.

A 2.3 mg single crystal of $HoVO_4$ was used for the magnetic susceptibility experiments, which were performed using a superconducting quantum interference device magnetometer over the temperature range of 10–320 K with an applied magnetic field of 500 G. The crystal was mounted on a quartz fiber, and the measurements were made with the applied magnetic-field direction both parallel and perpendicular to the fourfold crystallographic c axis.

III. RESULTS AND DISCUSSION

A. Inelastic neutron measurements

The low-Q neutron spectra in terms of the scattering function S, as obtained with incident-neutron energies of 5, 20, and 50 meV at temperatures between 15 and 100 K, are shown in Figs. 1–3. Contributions from phonon scattering are negligible in all of the spectra. From a 50-meV run of nonmagnetic $LuVO_4$, which shows only a flat nonmagnetic background in the corresponding low-Q regions, the phonon contribution is estimated to be less than 5% of the total intensity. The energy-transfer regions $E>0$ and $E<0$ correspond to neutron energy loss and energy gain, respectively. Transitions labeled X and $-X$ represent the Stokes (excitation) and anti-Stokes (deexcitation) lines, respectively. Magnetic peaks (labeled A to M) due to crystal-field transitions are identified at these energies in units of meV: 2.4 (A), 3.0 (D), 5.5 (B), 8.6 (G,J), 10.6 (K), 22.7 (H,L,M), 25.5 (E,F), and 32.5 (C).

Since $HoVO_4$ has a nonmagnetic singlet ground state and the next excited state is at 2.5 meV (29 K), elastic scattering at 15 K mainly consists of nuclear-incoherent and Bragg scattering. However, at elevated temperatures, transitions within the populated doubly degenerate states give rise to small additional elastic-magnetic intensities. The decrease in the intensity of peaks A, B, and C

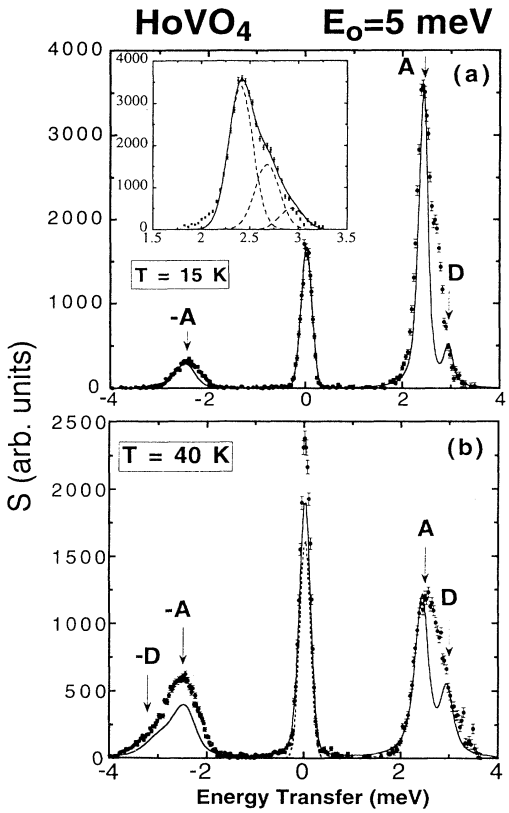

FIG. 1. The observed (solid circles) and calculated (solid curve) scattering functions for an incident energy of 5 meV as a function of energy transfer at (a) 15 K and (b) 40 K. The labels of the peaks correspond to the crystal-field transitions shown in Fig. 4(a). The calculated spectra were convoluted with the instrumental resolution function and corrected for the nuclear contribution to the elastic intensity. The inset indicates a small splitting of the first excited doublet state (see text).

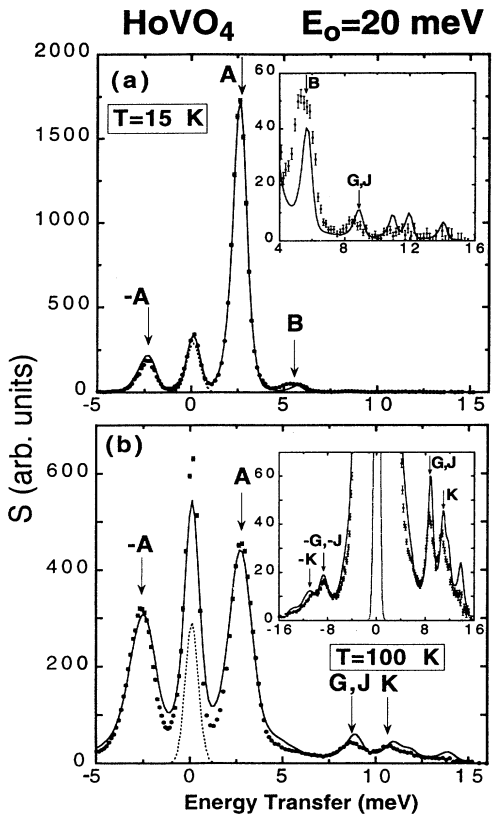

FIG. 2. The observed (solid circles) and calculated (solid curve) scattering functions for an incident energy of 20 meV at (a) 15 K and at (b) 100 K. The labels of the peaks correspond to the crystal-field transitions as shown in Fig. 4(a). The broken line indicates the nuclear contribution to the elastic peak. The weak transitions are shown in an expanded scale in the insets.

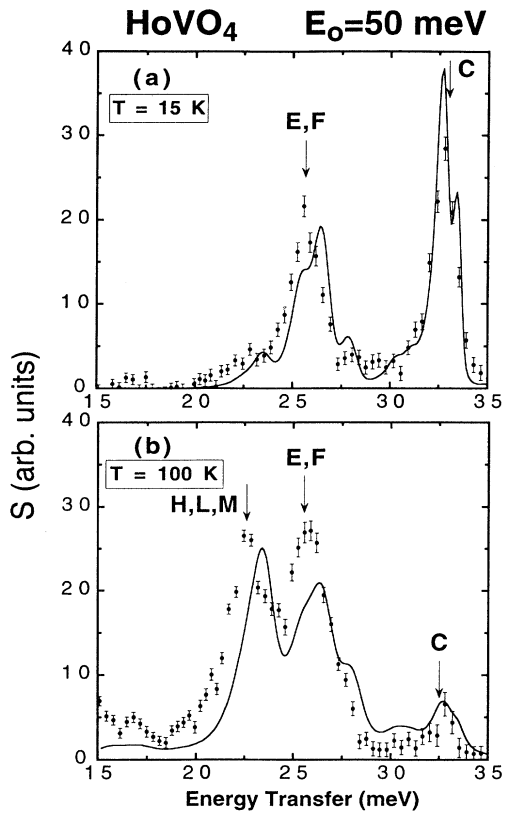

FIG. 3. The observed (solid circles) and calculated (solid curve) scattering functions for an incident energy of 50 meV at (a) 15 K and at (b) 100 K. The labels of the peaks correspond to the crystal-field transitions as shown in Fig. 4(a).

with increasing temperature indicates that these peaks originate from the ground state. Other peaks showing intensities of the opposite temperature dependence correspond to transitions from populated excited states. A careful analysis of all the spectra using a crystal-field model (as described below) led to a crystal-field-level scheme for the Ho^{3+} ground multiplet in $HoVO_4$ shown in Fig. 4(a).

B. Crystal-field analysis

The energies and intensities of the crystal-field transitions were obtained by a diagonalization of the full Hamiltonian, which consists of free-ion (H_{FI}) and crystal-field parts (H_{CF}), i.e.,

$$H = H_{FI} + H_{CF} , \tag{1}$$

using the scheme of intermediate coupling and by employing spherical-tensor techniques.[26] The crystal-field Hamiltonian can be written as

$$H_{CF} = \sum_{k,q,i} B_q^k [C_q^k(i) + C_{-q}^k(i)], \quad k \geq q \geq 0 , \tag{2}$$

where the $C_q^k(i)$ are spherical-tensor operators of rank k for the ith electron, and the summation is over all equivalent electrons in the f shell. The B_q^k are crystal-field parameters, and for the present D_{2d} point symmetry, five crystal-field parameters, B_0^2, B_0^4, B_0^6, B_4^4, and B_4^6 are needed to describe the interaction. The fitting procedure, selection rules, and self-consistency checks have been de-

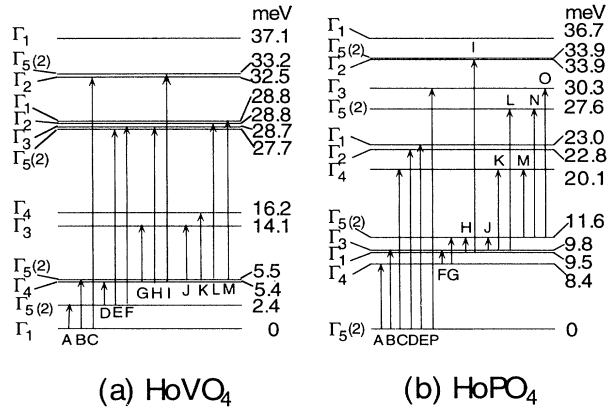

FIG. 4. The schematic diagram of the crystal-field splitting of the Ho^{3+} ground multiplet ($^5I_8$) in (a) $HoVO_4$ and (b) $HoVO_4$. The experimentally observed transitions are labeled by the letters.

scribed in detail in a previous study[19] of $HoPO_4$. Although there are only 17 states in the ground multiplet of a Ho^{3+} ion, the lowest 97 states of the f^{10} configuration were used in the matrix diagonalization so that mixing between the ground multiplet and the higher J multiplets, if any, is not affected by the energy truncation. For the free-ion parameters, the previously established values for a Ho^{3+} ion in a LaF_3 host[27] were used, and they remained fixed during the fitting process. The following criteria were used in the crystal-field parameter refinement.

(i) The assignments must obey the selection rules for magnetic-dipole transitions of magnetic neutron scattering.

(ii) The residual error is minimized for both the energy positions and transition intensities.

(iii) An overall satisfactory agreement is sought for all the spectra at different temperatures.

(iv) The calculated magnetic properties (e.g., magnetic susceptibility with the field directions parallel and perpendicular to the c axis) must agree reasonably well with the experimental values.

We find that the variation of crystal-field parameters is rather sensitive to the magnitudes of the transition matrix elements and the nature of the anisotropic magnetization. Therefore, (ii) and (iv) above are the most important conditions.

The lack of magnetic elastic intensity at 15 K [other than the nuclear incoherent scattering mainly from V, see Fig. 1(a)] confirms a nonmagnetic singlet ground state in $HoVO_4$. All the magnetic elastic intensity ($<4\%$ of total) was accounted for by the transition within the thermally occupied first doublet Γ_5. In addition, the rise of additional magnetic intensities at 40 and 100 K indicates the presence of two magnetic Γ_5 doublets at low energies (<10 meV). This basic subset of crystal-field levels is supported by optical and NMR data.[6–8] Based on this knowledge and the above criteria we conducted an extensive search for initial parameter sets using a Monte Carlo method. First, the excitation spectra corresponding to 350 000 random sets generated within a parameter space of $|B_0^2| \leq 1000$, $|B_0^4| \leq 1000$, $|B_0^6| \leq 1500$, $|B_4^4| \leq 1500$, and $|B_4^6| \leq 1000$ cm^{-1} were examined and 17 sets of the lowest residual errors were obtained. All subsequent fits to the experimental data using these initial parameters converged to a single minimum. As a check for possibly additional nearby local minima, another Monte Carlo search which generated 700 000 random parameter sets was conducted within a somewhat smaller parameter space from which over 400 sets were tested. None of these parameter sets was found to provide an equally good or better fit to the data. The optimized crystal-field parameters in units of cm^{-1} are $B_0^2=-164$, $B_0^4=302$, $B_0^6=-740$, $B_4^4=-890$, and $B_4^6=114$. They are in reasonable agreement with those obtained previously from an analysis of the susceptibility data by Guo and co-workers.[10] The calculated magnetic spectra, when convoluted with th spectrometer resolution, are shown by the solid lines in Figs. 1–3. They were normalized to the observed intensity of the 2.4-meV peak at 15 K except in the case of the $E_0=50$-meV spectra, where the intensities were normalized to the 32.5-meV peak at 15 K. The intrinsic widths of the peaks provide a measure of the extent of the interactions between Ho ions and their environment. The variation of the estimated intrinsic widths (1–6 cm^{-1}) with temperature from 15 to 100 K is quite reasonable for a typical insulating solid. The calculated energies and wave functions of the crystal-field states are compared with the experimental results in Table I. The root-mean-square energy deviation is 3 cm^{-1}. The calculated crystal-field-level scheme and symmetry labeling of the states are shown in Fig. 4(a).

The crystal-field splitting of $HoVO_4$ obtained in the present neutron-scattering study agrees well with the previous optical and NMR data,[6,8] although not more than four levels were reported in these studies. Barakat and Finn[8] reported the splitting of the Ho^{3+} $^5I_7$ multiplet in the energy range of 5120–5250 cm^{-1}. A calculation of these energy levels using our crystal-field parameters produced an agreement with their data to within a root-mean-square deviation of 15 cm^{-1}. The present crystal-field parameters also agree reasonably well with those obtained from magnetic-susceptibility and magnetization measurements by other workers.[10–12] Goto and co-

TABLE I. The observed and fitted energies and the wave functions of the ground-state multiplet $^5I_8$ of the Ho^{3+} ion in $HoVO_4$. Small ($<2\%$) components of the $|8,m\rangle$ states are not listed.

$^5I_8$	E^{obs} (cm^{-1})	E^{cal} (cm^{-1})	Wave functions
Γ_1	0.0	0.0	$0.94\|0\rangle-0.24(\|4\rangle+\|-4\rangle)$
Γ_5	19.5±0.3	19.5	$\pm0.90\|\pm1\rangle\mp0.37\|\mp3\rangle\mp0.21\|\pm5\rangle\pm0.13\|\mp7\rangle$
Γ_4	43.2±0.7	43.2	$0.67(\|2\rangle-\|-2\rangle)-0.24(\|6\rangle-\|-6\rangle)$
Γ_5	44.4±1.6	44.4	$\pm0.99\|\pm7\rangle\mp0.13\|\mp1\rangle$
Γ_3	113.7±1.1	113.7	$-0.69(\|6\rangle+\|-6\rangle)+0.17(\|2\rangle+\|-2\rangle)$
Γ_4	130.4±1.1	130.4	$-0.67(\|6\rangle-\|-6\rangle)-0.23(\|2\rangle-\|-2\rangle)$
Γ_5	226±4	223.2	$\mp0.85\|\pm5\rangle\pm0.54\|\mp3\rangle$
Γ_3	226±4	231.7	$0.68(\|2\rangle+\|-2\rangle)+0.17(\|6\rangle+\|-6\rangle)$
Γ_2	227±5	232.3	$0.71(\|8\rangle-\|-8\rangle)$
Γ_1	227±5	232.3	$-0.66(\|4\rangle+\|-4\rangle)-0.35\|0\rangle$
Γ_2	263±3	261.9	$0.71(\|4\rangle-\|-4\rangle)$
Γ_5		268.0	$0.76\|\pm3\rangle+0.50\|\mp5\rangle+0.42\|\mp1\rangle$
Γ_1		299.3	$-0.66(\|4\rangle+\|-4\rangle)-0.35\|0\rangle$

workers[14] have measured the temperature dependence of the elastic constants of $HoVO_4$ using an ultrasonic technique. The softening of the C_{11}, $(C_{11}-C_{12})/2$, and C_{66} elastic constants with decreasing temperature were attributed to an interaction between the quadrupolar moment of the Ho ions and the elastic strain. They obtained a set of simplified crystal-field parameters from a perturbation treatment assuming a bilinear quadrupole-strain coupling, however, their crystal-field parameters do not agree well with the present results. This is perhaps not surprising given the approximations employed in their treatment and the possibly strong correlation between the crystal-field parameters and the coupling constants.

Although, in general, while the experimental data are in fair agreement with the calculated spectra, an obvious discrepancy can be seen in the strongest transitions A and $-A$ in the high-resolution spectra of Fig. 1. Clearly, there are extra intensities centered at about 2.7 meV which are not accounted for by the crystal-field calculation. It can be seen from the inset of Fig. 1(a) that a "two-peak" structure separated by 2.3 cm^{-1} matches quite well the observed profile for transition A (excitation from the ground state to the first Γ_5 doublet). The same (but better resolved) splitting of the Γ_5 lines in the optical spectra was also observed by Battison and co-workers.[6] This splitting suggests a lowering of the local symmetry at the rare-earth site even though an overall "average" tetragonal structure is maintained. Apparently these local defects do not occur in diluted compounds since no splitting was observed in $Ho_{0.1}Y_{0.9}VO_4$,[6] and their influence to the other Γ_5 doublets, i.e., those at 5.5, 27.7, and 33.2 meV is much weaker.[28] The neutron data [Fig. 2(a)] show a width of the 5.5-meV excitation which is larger than that predicted by the crystal-field model, however, the resolution is not sufficient to confirm the existence of a splitting. Unlike the optical studies, neutron-scattering measurements provide additional information regarding the Q dependence of the splitting. We find that for $0.46 < Q < 0.64$ $Å^{-1}$, the relative intensity of the split components is about 2 to 1 favoring the lower-energy peak, whereas for $1.9 < Q < 2.5$ $Å^{-1}$, the two subpeaks have roughly the same intensity. Additional neutron-scattering investigations, perhaps requiring single-crystal measurements [as in the case of $TmVO_4$ (Ref. 29)] are needed in order to clarify the nature of this splitting.

C. Magnetic properties and comparison with $HoPO_4$

Using the present crystal-field results we have calculated the Van Vleck paramagnetic susceptibility[30] for $HoVO_4$ and the results are shown in Fig. 5. The agreement between the calculated and observed magnetic susceptibility over the 10–300 K temperature range is excellent for both field directions. The good agreement in the 10 K region indicates a negligible Ho spin-spin correlation because of the nonmagnetic ground state. A strong anisotropy favoring an easy plane perpendicular to the c axis is seen at temperatures below about 50 K. This anisotropy arises from the first excited doublet Γ_5 at about 2.5 meV, which shows calculated spectroscopic g factors

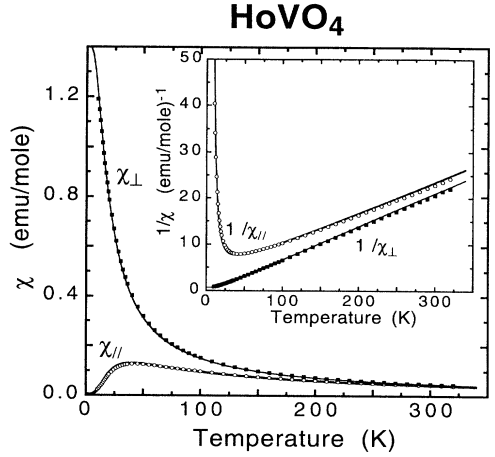

FIG. 5. The temperature dependence of the measured (symbols) and calculated (lines) magnetic susceptibilities and inverse susceptibilities (inset) for $HoVO_4$ with the field direction parallel ($\chi_\parallel$) and perpendicular ($\chi_\perp$) to the crystallographic c axis.

of $g_\parallel = 1.3$ and $g_\perp = 0$ for an effective spin of $\frac{1}{2}$. (The symbols $\parallel$ and $\perp$ represent the direction of the applied magnetic field parallel and perpendicular to the c axis, respectively.) The difference in the matrix elements of the magnetic moment (in units of Bohr magnetons) between the ground state Γ_1 and the first excited state Γ_5, i.e., $|\langle \Gamma_5|\mu_\parallel|\Gamma_1\rangle| = 0$ versus $|\langle \Gamma_5|\mu_\perp|\Gamma_1\rangle| = 5.1$, gives rise to this magnetic anisotropy in $HoVO_4$ at low temperatures.

The important role of crystal-field effects in influencing the magnetic behavior is nicely illustrated by a comparison of the $HoVO_4$ and $HoPO_4$ characteristics. In Fig. 4(b) the crystal-field scheme of Ho in $HoPO_4$ obtained from a previous study[19] is illustrated. $HoPO_4$ has a magnetic-doublet ground state consisting of a 98% $|8,7\rangle$ component, and the higher states lie above 8 meV. Consequently, $HoPO_4$ exhibits a low-temperature magnetic anisotropy which is opposite to that of $HoPO_4$, i.e., $\chi_\parallel/\chi_\perp = 45$ at 5 K, thereby favoring an easy magnetization axis along the c direction. At 1.35 K, indirect dipole-dipole interactions between the Ho moments apparently lead to a long-range antiferromagnetic ordering with the moments parallel/antiparallel to the c axis. $HoVO_4$ lacks such an interaction due to the nonmagnetic ground state, and the Ho moments show no ordering down to mK temperatures. The difference in crystal-field structure of these two materials also manifests itself in the magnetic specific heat where the Schottky maximum in $HoPO_4$ is displaced to higher temperatures as compared with $HoVO_4$.

The physical origin of the different crystal-field splitting in these isostructural compounds is relatively complex. A salient feature in comparing the crystal-field parameters is the opposite sign of the B_0^2 parameter, i.e., -164 cm^{-1} for $HoVO_4$ versus 402 cm^{-1} for $HoPO_4$. Since the $B_0^2 C_0^2$ term represents the quadrupolar effect of the crystal fields, this suggests that the quadrupole interactions in these two materials are intrinsically

different. If the quadrupolar moments of the Ho^{3+} ground state couple to the crystal lattice, then the resulting lattice properties of $HoVO_4$ and $HoPO_4$ should behave differently. An anomalous and opposite temperature dependence between the $HoVO_4$ and $HoVO_4$ lattice parameters, a and c, has indeed been observed from a neutron-diffraction study of the $HoV_xP_{1-x}O_4$ system. The results of this study have been given in a separate work.[20]

The different magnetic properties and crystal-field structures between the RPO_4 and RVO_4 compounds have been found by several researchers.[31–34] (Only the heavy rare earths from Tb to Lu in the RPO_4 series form the zircon structure.) So far, there is no satisfactory explanation of this phenomenon, however, only a few systematic investigations devoted to the characterization of the ground-states and lattice properties of these series have been carried out at this time. Accordingly, a systematic study of the contrasting physical properties in these materials by various spectroscopic techniques is currently under way.

IV. CONCLUSIONS

The dynamic and static magnetic properties of $HoVO_4$ have been studied using neutron-scattering and magnetic-susceptibility measurements. The neutron data, as analyzed by a single-ion crystal-field model, led to the determination of a set of crystal-field parameters for the Ho^{3+} ions. The calculated magnetic spectra and susceptibility based on the refined crystal-field parameters provide an adequate overall description of the experimental data. The magnetic properties between $HoVO_4$ and $HoVO_4$ were compared and this comparison emphasized some of the contrasting behavior. Most of the single-ion magnetic properties at low temperatures can be explained by the different crystal-field structure and ground-state wave functions of these two compounds. The present characterization of the ground-state wave functions provides a basis for future extended studies of more-complex phenomena which involve interactions among the rare-earth ions and/or between the $4f$ electrons and the crystal lattice.

ACKNOWLEDGMENTS

Research at the Argonne National Laboratory and the Oak Ridge National Laboratory was supported, respectively, by the Department of Energy, Basic Energy Sciences, under Contract No. W-31-109-ENG-38, and by Contract No. DE-AC05-84OR21400 with Martin Marietta Energy Systems, Inc.

[1]B. C. Chakoumakos, M. M. Abraham, and L. A. Boatner, J. Solid State Chem. **109**, 197 (1994).
[2]J. A. Wunderlich, J. G. Sliney, and L. G. DeShazer, IEEE J. Quantum Electron **13**, 69 (1977).
[3]A. K. Levine and F. C. Palilla, Appl. Phys. Lett. **5**, 118 (1964).
[4]R. T. Harley, in *Spectroscopy of Solids Containing Rare Earth Ions,* edited by A. Kapyanskii and R. M. Macfarlane (Elsevier, Amsterdam, 1987), p. 557.
[5]G. A. Gehring and K. A. Gehring, Rep. Prog. Phys. **38**, 1 (1975).
[6]J. E. Battison, A. Kasten, M. J. M. Leask, and J. B. Lowry, J. Phys. C **10**, 323 (1977); J. E. Battison, A. Kasten, M. J. M. Leask, and J. B. Lowry, Phys. Lett. **55A**, 173 (1975).
[7]H. Bischoff, B. Pilawa, A. Kasten, and H. G. Kahle, J. Phys. Condens. Matter **3**, 10057 (1991); B. Pilawa, S. Müller, and H. G. Kahle, *ibid.* **6**, 461 (1994).
[8]M. Barakat and C. B. P. Finn, J. Phys. C **21**, 6123 (1988).
[9]P. J. Becker and G. A. Gehring, Solid State Commun. **16**, 795 (1975).
[10]M.-D. Guo, A. T. Aldred, and S.-K. Chan, J. Phys. Chem. Solids **48**, 229 (1987).
[11]S. I. Andronenko, A. N. Bazhan, V. A. Loffe, and Yu. P. Udalov, Fiz. Teverd. Tela (Leningrad) **27**, 609 (1985) [Sov. Phys. Solid State **27**, 379 (1985)].
[12]V. A. Loffe, S. I. Andronenko, A. N. Bazhan, S. V. Kravchenko, C. Bazan, B. G. Vekhter, and M. D. Kaplan, Zh. Eksp. Teor. **84**, 707 (1983) [Sov. Phys. JETP **57**, 408 (1983)].
[13]B. Bleaney, F. N. H. Robinson, and M. R. Wells, Proc. R. Soc. London A **362**, 179 (1978).
[14]T. Goto, A. Tamaki, T. Fujimura, and H. Unoki, J. Phys. Soc. Jpn. **55**, 1613 (1986).
[15]H. Suzuki, T. Ohtsuka, S. Kawarazaki, N. Kunitomi, R. M. Moon, and R. M. Nicklow, Solid State Commun. **49**, 1157 (1984).
[16]R. M. Nicklow, R. M. Moon, S. Kawarazaki, N. Kunitomi, H. Suzuki, T. Ohtsuka, and Y. Morii, J. Appl. Phys. **57**, 3784 (1985).
[17]M. Steiner, K. Siemensmeyer, K. D. Ohlhoff, G. Rahn, M. Kubota, and S. H. Smith, J. Magn. Magn. Mater. **54**, 1333 (1986).
[18]S. Kawarazaki and J. Arthur, Physica B **136**, 379 (1989).
[19]C.-K. Loong, L. Soderholm, J. P. Hammonds, M. M. Abraham, L. A. Boatner, and N. M. Edelstein, J. Phys. Condens. Matter **5**, 5121 (1993).
[20]S. Skanthakumar, C.-K. Loong, L. Soderholm, J. Nipko, J. W. Richardson, Jr., M. M. Abraham, and L. A. Boatner, J. Alloys Compounds (to be published); S. Skanthakumar, C.-K. Loong, L. Soderholm, J. W. Richardson, Jr., M. M. Abraham, and L. A. Boatner, Phys. Rev. B **51**, 5644 (1995).
[21]M. M. Abraham, L. A. Boatner, T. C. Quinby, D. K. Thomas, and M. Rappaz, Radioact. Waste Manage. **1**, 181 (1981).
[22]C.-K. Loong, S. Ikeda, and J. M. Carpenter, Nucl. Instrum. Methods A **260**, 381 (1987).
[23]C.-K. Loong, L. Soderholm, M. M. Abraham, L. A. Boatner, and N. M. Edelstein, J. Chem. Phys. **98**, 4214 (1993).
[24]C.-K. Loong, L. Soderholm, G. L. Goodman, M. M. Abraham, and L. A. Boatner, Phys. Rev. B **48**, 6124 (1993).
[25]C.-K. Loong and L. Soderholm, J. Alloys Compounds **207/208**, 153 (1994).
[26]H. M. Crosswhite and H. Crosswhite, J. Opt. Soc. Am. B **1**, 246 (1984).
[27]W. T. Carnall, G. L. Goodman, K. Rajnak, and R. S. Rana, J. Chem. Phys. **90**, 3443 (1989).
[28]B. Pilawa (private communication).
[29]J. K. Kjems, W. Hayes, and S. H. Smith, Phys. Rev. Lett. **35**, 1089 (1975).

[30]J. H. Van Vleck, in *The Theory of Electric and Magnetic Susceptibilities* (Oxford University Press, London, 1932).
[31]C. Linares, A. Louat, and M. Blanchard, Struct. Bonding (Berlin) **33**, 179 (1977).
[32]D. J. Newman and G. E. Stedman, J. Phys. Chem. Solids **32**, 535 (1971).
[33]Vishwamittar and S. P. Puri, Phys. Rev. B **9**, 4673 (1974).
[34]C. A. Morrison and R. P. Leavitt, in *Handbook on the Physics and Chemistry of Rare Earths,* edited by K. A. Gschneidner, Jr. and I. Eyring (North-Holland, Amsterdam, 1982), p. 461.